

Electronic supplementary information (ESI)

Realization of deep-blue TADF in sterically controlled naphthyridines for vacuum- and solution-processed OLEDs

Gediminas Kreiza^a, Dovydas Banovičius^a, Justina Jovaišaitė^a, Saulius Juršėnas^a, Tomas Javorskis^b, Vytenis Vaitkevičius^b, Edvinas Orentas^b, Karolis Kazlauskas*^a

E-mail: karolis.kazlauskas@ff.vu.lt

^aInstitute of Photonics and Nanotechnology, Vilnius University, Saulėtekio av. 3, LT-10257 Vilnius, Lithuania

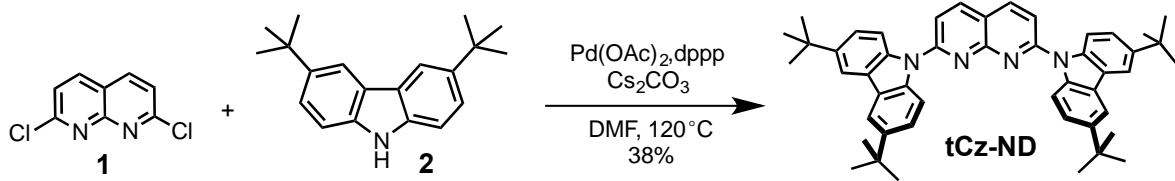
^bDepartment of Organic Chemistry, Vilnius University, Faculty of Chemistry and Geosciences, Naugarduko 24, Vilnius LT-03225, Lithuania

Synthesis and identification

All reagents and starting materials were obtained from commercial sources and used as received. Reaction solvents, dimethylformamide was distilled from CaH₂, THF was distilled from sodium/ benzophenone. All moisture-sensitive reactions were performed in oven-dried (230 °C) glassware under an atmosphere of dry argon. Thin-layer chromatography was performed on Merck silica gel plates with QF-254 indicator. Visualization was accomplished with UV (254 nm), potassium permanganate (KMnO₄), ninhydrin or vanillin. Column chromatography was performed using Merck silica 60 (40–63 µm particle size). ¹H and ¹³C NMR spectra were recorded on a NMR spectrometer at 400 MHz for ¹H and 101 MHz for ¹³C, respectively. ¹H and ¹³C NMR spectra are referenced to residual solvent (CDCl₃, 7.29 and 77.16 ppm for ¹H NMR and ¹³C NMR, respectively). When necessary, assignments were obtained by reference to COSY, HSQC, and HMBC correlations. Chemical shifts are reported in ppm, and multiplicities are indicated by br (broad), s (singlet), d (doublet), t (triplet), q (quartet), quint (quintet), sxt (sextet), sept (septet), m (multiplet), and combinations thereof. Infrared (IR) spectra were recorded on a FTIR spectrometer equipped with a diamond ATR unit. Melting points were determined in open capillary tubes and are uncorrected. HRMS was recorded on Bruker Daltonics microTOF-II spectrometer equipped with ESI ion source in positive mode.

2,7-dichloro-1,8-naphthyridine **1**¹ and 1-bromo-3,6-di-*tert*-butyl-9*H*-carbazole **4**² were synthesized according to literature.

Abbreviations: DCM, dichloromethane; DMF, dimethylformamide; dppp, 1,3-bis(diphenylphosphino)propane; EtOAc, ethyl acetate; PE, petrol ether (40–60 °C fraction).



Pd(OAc)₂ (12.2 mg, 5 mol %) and 1,3-bis(diphenylphosphino)propane (dppp) (41.2 mg, 5 mol %) was dissolved in 10 ml DMF at room temperature. After 5 min, 2,7-dichloro-1,8-naphthyridine **1** (100 mg, 1.0 mmol, 1.0 equiv.), 3,6-di-tert-butyl-9H-carbazole **2** (765 mg, 3.0 mmol, 3.0 equiv.) and cesium carbonate (1.63 g, 5.0 mmol, 5.0 equiv.) were added. The reaction mixture was heated at 120 °C for 48 h. Reaction was quenched with water. After extraction with CHCl₃, the crude product was purified by column chromatography (EtOAc/PE 1:60) to afford 263 mg (38%) of **tCz-ND** as a light-yellow solid.

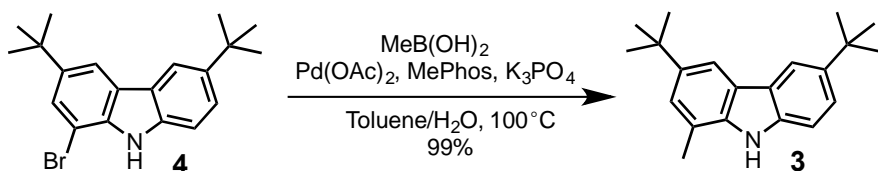
R_f = 0.4 (1/20 EtOAc:PE), m.p. >280°C.

¹H NMR (400 MHz, CDCl₃) δ 8.36 (d, *J*=8.5, 2H), 8.24 (d, *J*=8.7, 4H), 8.15 (d, *J*=1.9, 4H), 7.96 (d, *J*=8.5, 2H), 7.57 (dd, *J*=8.7, 2.0, 4H), 1.51 (s, 36H) ;

¹³C NMR (100 MHz, CDCl₃) δ 155.9, 154.8, 144.8, 138.6, 137.7, 125.2, 124.22, 118.2, 116.8, 116.1, 112.2, 34.8, 31.9;

IR: $\nu_{\text{max}}/\text{cm}^{-1}$ 2954, 1470, 1360, 808;

HRMS (ESI) calc. for C₄₈H₅₃N₄ (M+H): 685.4265; Found: 685.4264.

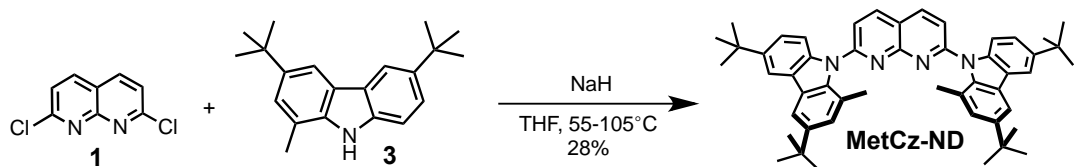


Reaction tube was charged with 1-bromo-3,6-di-*tert*-butyl-9*H*-carbazole **4** (320 mg, 0.893 mmol, 1.0 equiv.), methylboronic acid (134 mg, 2.239 mmol, 2.5 equiv.), tribasic potassium phosphate (0.76g, 3.58 mmol, 4 equiv.), Pd(OAc)₂ (10 mg, 0.045 mmol, 0.05 equiv.) and MePhos (33 mg, 0.091 mmol, 0.1 equiv.) under argon. Next, degassed solution of toluene/H₂O (3:1, 10 ml) was added. Screw-capped tube was heated at 100°C for 48h. Filtration through celite pad with EtOAc and purification by column chromatography on silica gel DCM/PE (1:5) afforded 259 mg (99%) of **3** as a yellowish oil.

R_f = 0.29 (1/5 DCM:PE).

¹H NMR (400 MHz, CDCl₃) δ 8.08-8.10 (m, 1H), 7.94-7.96 (m, 1H), 7.80 (s, 1H), 7.47-7.50 (m, 1H), 7.38-7.41 (m, 1H), 7.29-7.31 (m, 1H), 2.58 (s, 3H), 1.48 (s, 9H), 1.47 (s, 9H);

¹³C NMR (100 MHz, CDCl₃) δ 142.5, 142.2, 138.0, 137.5, 124.3, 123.8, 123.4, 122.8, 118.9, 116.3, 113.7, 110.1, 34.7, 34.6, 32.1, 32.0, 17.2;
IR: ν_{max}/cm⁻¹ 3421, 2951, 1493, 1296, 865, 805;
HRMS (ESI) calc. for C₂₁H₂₈N (M+H): 294.2216; Found: 294.2208.



To a solution of **3** (161 mg, 0.549 mmol, 2.2 equiv.) in freshly distilled THF (8.0 ml) NaH (60% dispersion in mineral oil) (30 mg, 0.75 mmol, 3.0 equiv.) was added in one portion under argon. Next, mixture was stirred at 55–60°C for 1.5 h and subsequently cooled to r.t. Afterwards **1** (49 mg, 0.249 mmol, 1.0 equiv.) was added in one portion, tube was screw-capped and heated at 105°C for 96h. Purification by column chromatography on silica gel 1/30 (EtOAc:PE) afforded 49 mg (28%) of **MetCz-ND** as a yellowish solid.

R_f = 0.31 (1/20 EA:PE), m.p. >300°C.

¹H NMR (400 MHz, CDCl₃) δ 8.34 (d, J= 8.4 Hz, 2H), 8.10-8.12 (m, 2H), 8.00-8.02 (m, 2H), 7.92 (d, J= 8.4 Hz, 2H), 7.54 (d, J= 8.4 Hz, 2H), 7.46-7.50 (m, 2H), 7.31-7.33 (m, 2H), 2.29 (s, 6H), 1.50 (s, 18H), 1.48 (s, 18H); **¹³C NMR** (100 MHz, CDCl₃) δ 155.6, 155.0, 144.7, 144.6, 140.1, 137.8, 137.7, 127.1, 126.2, 125.0, 124.1, 122.1, 120.7, 119.3, 116.0, 114.0, 111.1, 34.8, 34.6, 31.9, 29.7, 21.3;

IR: ν_{max}/cm⁻¹ 2952, 1491, 1446, 1230, 867, 806;

HRMS (ESI) calc. for C₅₀H₅₇N₄ (M+H): 713.4578; Found: 713.4577.

X-Ray Crystallography

Single crystals of the investigated compounds were grown from DMF solutions by slow evaporation method. Suitable crystals were selected and mounted on a nylon loop in inert oil and analyzed on a XtaLab Synergy diffractometer equipped with HyPix-6000HE hybrid photon counting detector and PhotonJet microfocus X-ray source delivering CuKα ($\lambda = 1.54184$) radiation. X-ray measurements were carried out at 100.0 K using Oxford Cryostream 800 cooling system. Data were collected and processed using CrysAlisPro software. Employing Olex2 graphical interface,³ the structures were solved by Intrinsic Phasing with the ShelXT⁴ program and refined with the ShelXL⁵ package using Least Squares minimization. It is worth noting that highly disordered solvent molecules in **MetCz-ND** crystal lattice were present. To remove the electronic contribution of solvent molecules from the refinement, solvent masking was applied. The structure files of **tCz-ND** and **MetCz-ND** crystals were deposited with the Cambridge Crystallographic Data Centre (CCDC **1991494**; **1992697**).

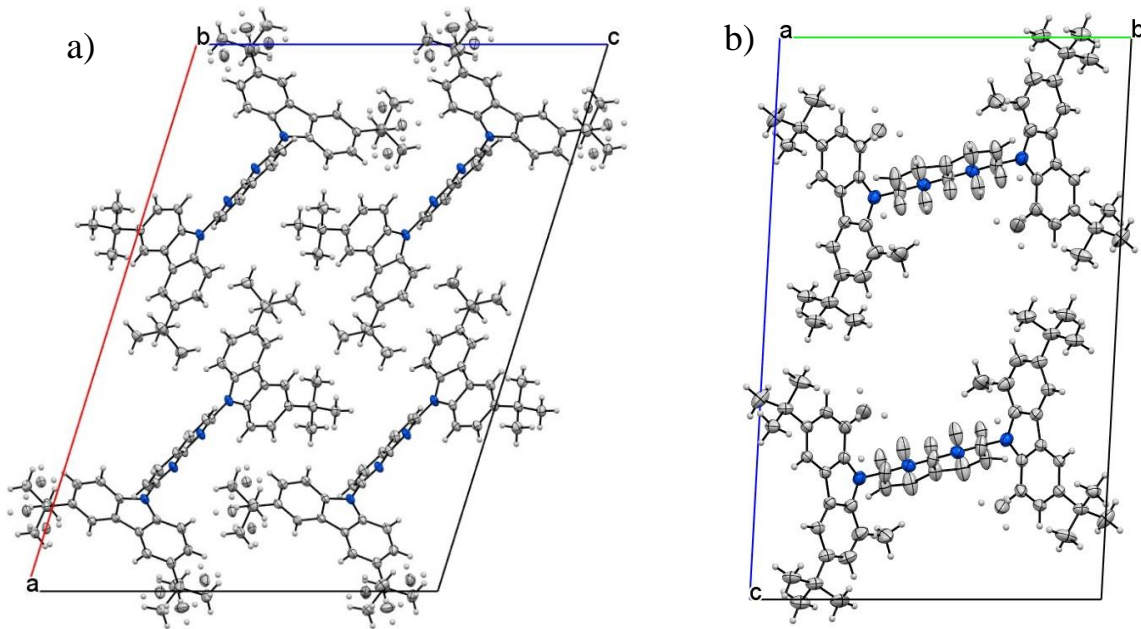


Figure S1. Illustration of unit cell contents obtained by XRD measurements: a) view down crystallographic axis b of **tCz-ND**; b) view down crystallographic axis a of **MetCz-ND**. Thermal ellipsoids are at 50% probability level.

Table S1. Crystallographic data of **tCz-ND** and **MetCz-ND** crystals.

Compound	tCz-ND	MetCz-ND
Formula	C ₄₈ H ₅₂ N ₄	C ₅₀ H ₅₆ N ₄
$\rho_{calc.}/\text{g cm}^{-3}$	1.181	0.963 + solvent
μ/mm^{-1}	0.524	0.425
Formula Weight	684.93	712.98
Colour	yellow	yellow
Shape	needle	needle
Size/mm ³	0.51×0.05×0.04	0.70×0.06×0.05
T/K	100.00(13)	99.99(11)
Crystal System	monoclinic	triclinic
Space Group	P2 ₁ /c	P-1
a/Å	30.1012(6)	5.94900(10)
b/Å	6.18300(10)	16.31420(10)
c/Å	21.6823(4)	25.8129(2)
$\alpha/^\circ$	90	93.0010(10)
$\beta/^\circ$	107.347(2)	90.0120(10)
$\gamma/^\circ$	90	100.5010(10)
V/Å ³	3851.87(13)	2459.77(5)
Z	4	2
Z'	1	1
Wavelength/Å	1.54184	1.54184
Radiation type	Cu K _a	Cu K _a
$\Theta_{min}/^\circ$	3.076	2.759
$\Theta_{max}/^\circ$	71.879	76.681
Measured Reflections	21090	44637
Independent Reflections	7334	9455
Reflections with I > 2(I)	6200	7558
R_{int}	0.0245	0.0319
Parameters	544	570
Restraints	0	0
Largest Peak	0.212	0.402
Deepest Hole	-0.202	-0.194
Goodness-of-fit	1.039	1.066
wR ₂ (all data)	0.1115	0.1792
wR ₂	0.1066	0.1709
R ₁ (all data)	0.0497	0.0660
R ₁	0.0410	0.0568

Thermal stability

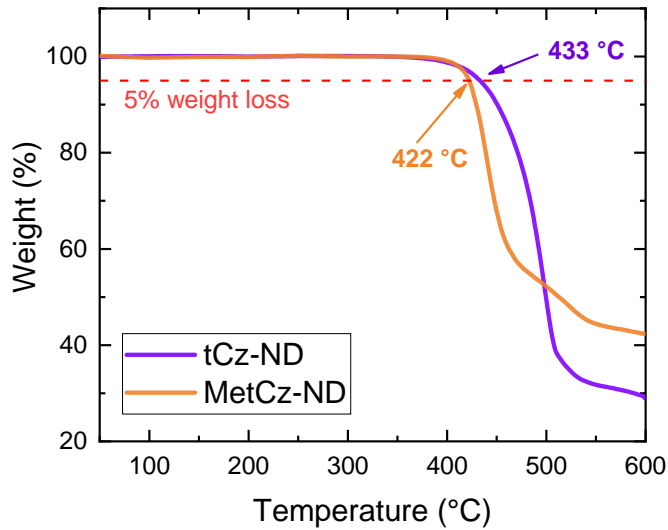


Figure S2. TGA traces of **tCz-ND** and **MetCz-ND** recorded at 10 K/min heating rate in N₂ environment. Thermal decomposition temperatures corresponding to 5% weight loss are indicated.

DFT calculations

Ground state geometries were optimized in vacuum by employing density functional theory (DFT) with B3LYP functional at 6-31G(d) basis set as implemented in Gaussian 09W software.⁶ Time dependent DFT method at the same basis set level was used to calculate ground to excited state transition energies (*E*), oscillator strengths (*f*) and to obtain HOMO and LUMO orbitals.

Table S2. Data obtained from TD-DFT calculations at B3LYP/6-31G(d) level by using optimized ground state geometry at the same basis set.

Compound	$E_{S0 \rightarrow S1}$ (eV)	$f_{[S_0 \rightarrow S_1]}$	$E_{S0 \rightarrow S2}$ (eV)	$f_{[S_0 \rightarrow S_2]}$	$E_{S0 \rightarrow T1}$ (eV)	$E_{S0 \rightarrow T2}$ (eV)	$\angle tCz/ND^a$ (deg)	ΔE_{S1-T1} (eV)
tCz-ND	2.9056	0.4963	3.1734	0.0274	2.5559	2.7612	31	0.3497
MetCz-ND	2.7041	0.3100	2.8937	0.0241	2.465	2.6106	55	0.2391

^a dihedral angle between carbazole and naphthyridine

Photophysical properties

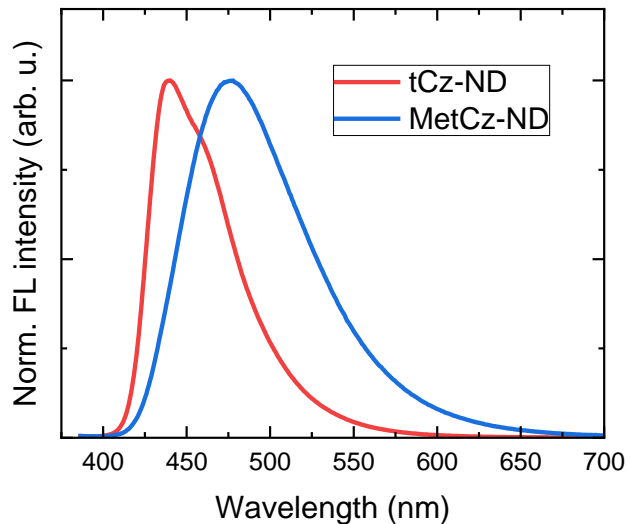


Figure S3. FL spectra of naphthyridine derivatives in toluene solutions (10^{-5} mol/l) at room temperature.

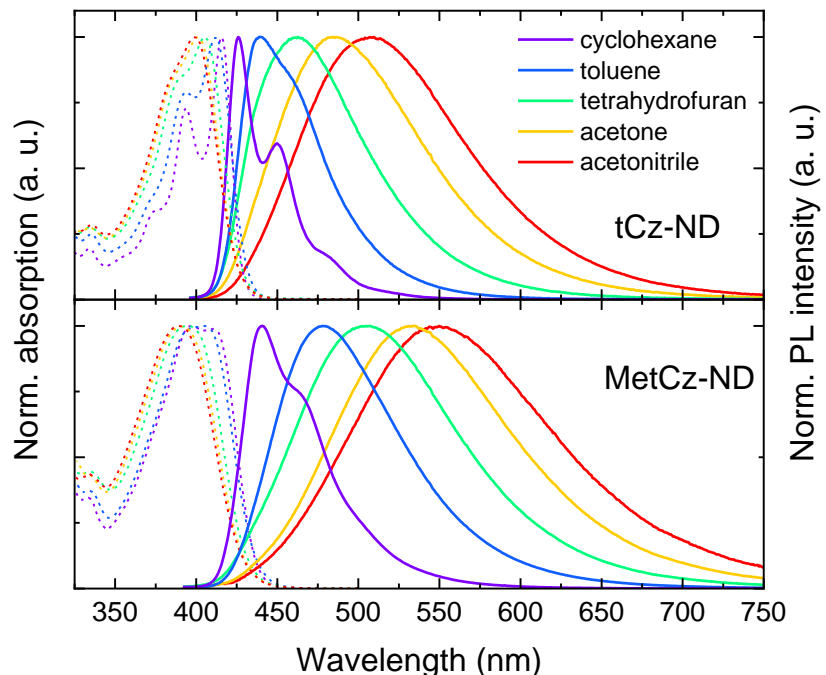


Figure S4. Absorption and FL spectra of naphthyridine derivatives in solvents of different polarity. Solution concentration $c = 10^{-5}$ mol/l.

Table S3. Photophysical properties of naphthyridine compounds in toluene (10^{-5} mol/l) and mCP host (7 wt%)

	Compound	λ_{max} (nm)	Φ_{FL}	$\Phi_{\text{DF}}/\Phi_{\text{PF}}$	τ_{PF} (ns)	τ_{DF} (μs)	k_r (10^6 s $^{-1}$)	$k_{\text{rISC}}^{\text{a}}$ (10^6 s $^{-1}$)	$k_{\text{ISC}}^{\text{a}}$ (10^7 s $^{-1}$)
Toluene	tCz-ND	440	0.53	0.26	4.0	2.8	104.2	0.16	14.4
	MetCz-ND	477	0.64	0.49	12.1	1.1	35.4	0.81	4.7
7 wt% In mCP	tCz-ND	452	0.76	2.3	5.2	8.8	44.2	0.34	14.8
	MetCz-ND	478	0.86	2.44	8.3	3.1	30.1	1.06	9.0

^a ISC (k_{ISC}) and rISC (k_{rISC}) rates were calculated according to the previously described procedures⁷ assuming that non-radiative decay occurs mainly from the triplet states as determined from the data in Figure 4.

OLED performance

Table S4. Main parameters of vacuum- and solution-processed OLEDs based on the naphthyridine TADF emitters (7 wt% in mCP).

Tech.	Emitter	V_{on} (V)	Maximum values				@100 cd/m ²			@1000 cd/m ²			CIE (x, y)	λ_{max} (nm)	FWHM (nm)		
			EQE (%)	L (cd/m ²)	CE (cd/A)	LE (lm/W)	Voltage (V)	EQE (%)	CE (cd/A)	LE (lm/W)	Voltage (V)	EQE (%)	CE (cd/A)	LE (lm/W)			
Vac	tCz-ND	3.25	17.01	8424	22.17	19.88	4.50	9.89	13.41	9.44	6.20	7.00	9.30	4.72	0.14, 0.16	459	66
Sol	tCz-ND	4.3	13.45	6840	17.26	10.24	6.50	12.11	15.84	7.64	8.55	7.80	9.80	3.48	0.15, 0.14	452	66
Vac	MetCz-ND	3.25	17.60	21459	31.98	23.60	4.50	14.43	25.46	17.76	5.87	12.50	24.72	13.2	0.18, 0.32	481	88
Sol	MetCz-ND	3.4	11.66	23028	23.84	11.76	4.87	7.5	14.75	9.80	6.12	11.00	22.80	11.6	0.16, 0.29	479	80

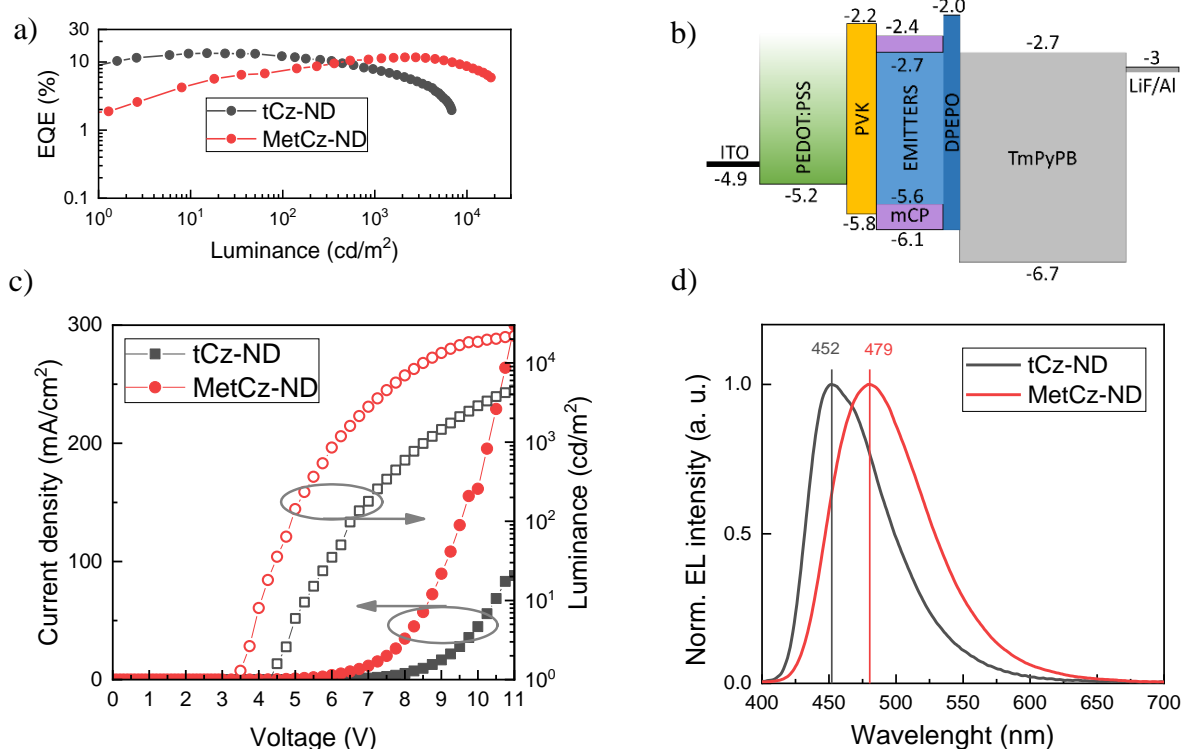


Figure S5. Characteristics of solution-processed OLEDs based on the naphthyridine TADF emitters dispersed in mCP host at 7 wt%: a) EQE vs luminance, b) energy level diagram, c) current density and luminance vs applied voltage, d) normalized electroluminescence spectra.

Table S5. Summarized main EL parameters of the best performing deep-blue ($\lambda_{\text{max}} < 460$ nm) TADF OLEDs reported in literature.

Compound	λ_{max} (nm)	CIE (x; y)	FWHM (nm)	EQE_{max} (%)	$\text{EQE} (\%) @ 100 \text{ cd/m}^2$	$\text{EQE} (\%) @ 1000 \text{ cd/m}^2$	Reference
tCz-ND (vacuum processed)	459	(0.14; 0.16)	66	17.0	9.9	7.1	This work
tCz-ND (solution processed)	452	(0.15; 0.14)	66	13.45	12.11	7.8	This work
34CzBN	458	(0.14; 0.14)	63	15.2	7.3	-	8
DCzBN2	436	(0.15; 0.07)	66	7.7	-	-	9
DCzBN3	428	(0.16; 0.06)	65	10.3	-	-	9
CNICCz	449	(0.15; 0.08)	56	12.4	6.4	-	10
CNICtCz	456	(0.14; 0.13)	60	16.0	10.7	-	10
DTTSAF	448	(0.15; 0.10)	68	6.2	~4.6	-	11
BDTPDDA	456	(0.14; 0.12)	56	8.5	~6.6	4.6	11
ICzAc	454	(0.15; 0.09)	56	13.7	-8	-	12
i-2CzdOXDMe	452	(0.17; 0.17)	85	11.8	1.3	-	13
DPAc-DdtCzBN	456	(0.16; 0.15)	67	23.1	18.3	-	14
TXAZ	456	(0.15; 0.13)	69	16.0	8.48	-	15
pDTCz-3DPyS	452	(0.15; 0.13)	~75	13.4	4.5	-	16
CzMeoB	455	(0.14; 0.10)	~50	16.1	12.4	-	17
TDBA-Ac	448	(0.15; 0.06)	48	21.5	~18	9.6	18
DMAC2PTO	448	(0.15; 0.11)	52	15.2	~5	-	19
PhICzACD	454	(0.16; 0.12)	51	17.0	6.4	-	20
DtBuAc-DBT	455	(0.13; 0.13)	84	10.5	9.8	-	21
OBA-O	446	(0.17; 0.17)	~100	17.8	15.5	8.5	22
Cz-TRZ4	446	(0.15; 0.10)	~70	18.3	-	~9	23
tCbz-mPYRs	441	(0.16; 0.12)	80	8.7	2.0	-	24
DCzTrz	459	(0.15, 0.15)	~60	17.5	~16	~11	25
DMTDAc	451	(0.15; 0.13)	65	19.8	19.8	~12	26
DMOC-DPS	460	(0.16; 0.16)	~80	14.5	9.0	3.7	27
Ac-3MHPM	451	(0.16; 0.15)	~75	17.8	10.4	-	28
FA-TA	454	(0.15; 0.13)	~70	11.2	-	-	29
3b	436	(0.16; 0.08)	~60	8.5	8.4	7.7	30
2CzdOXDPh	455	(0.16; 0.15)	75	6.8	2	1.4	31
TN4T-PCZ	~410	(0.16; 0.03)	~70	20.4	~12	20	32

References

- 1 G. R. Newkome, S. J. Garbis, V. K. Majestic, F. R. Fronczek and G. Chiarilc, *J. Org. Chem.*, 1981, **46**, 833–839.
- 2 C. Maeda, T. Todaka, T. Ueda and T. Ema, *Chem. - A Eur. J.*, 2016, **22**, 7508–7513.
- 3 O. V. Dolomanov, L. J. Bourhis, R. J. Gildea, J. A. K. Howard and H. Puschmann, *J. Appl. Crystallogr.*, 2009, **42**, 339–341.
- 4 G. M. Sheldrick, *Acta Crystallogr. Sect. A Found. Crystallogr.*, 2015, **71**, 3–8.
- 5 G. M. Sheldrick, *Acta Crystallogr. Sect. C Struct. Chem.*, 2015, **71**, 3–8.
- 6 M. J. Frisch, G. W. Trucks, H. B. Schlegel, G. E. Scuseria, M. A. Robb, J. R. Cheeseman, G. Scalmani, V. Barone, G. A. Petersson, H. Nakatsuji, X. Li, M. Caricato, A. Marenich, J. Bloino, B. G. Janesko, R. Gomperts, B. Mennucci, H. P. Hratchian, J. V. Ortiz, A. F. Izmaylov, J. L. Sonnenberg, D. Williams-Young, F. Ding, F. Lipparini, F. Egidi, J. Goings, B. Peng, A. Petrone, T. Henderson, D. Ranasinghe, V. G. Zakrzewski, J. Gao, N. Rega, G. Zheng, W. Liang, M. Hada, M. Ehara, K. Toyota, R. Fukuda, J. Hasegawa, M. Ishida, T. Nakajima, Y. Honda, O. Kitao, H. Nakai, T. Vreven, K. Throssell, J. J. A. Montgomery, J. E. Peralta, F. Ogliaro, M. Bearpark, J. J. Heyd, E. Brothers, K. N. Kudin, V. N. Staroverov, T. Keith, R. Kobayashi, J. Normand, K. Raghavachari, A. Rendell, J. C. Burant, S. S. Iyengar, J. Tomasi, M. Cossi, J. M. Millam, M. Klene, C. Adamo, R. Cammi, J. W. Ochterski, R. L. Martin, K. Morokuma, O. Farkas, J. B. Foresman and D. J. Fox, 2016.
- 7 G. Kreiza, D. Banovičius, J. Jovaišaitė, K. Maleckaitė, D. Gudeika, D. Volyniuk, J. V. Gražulevičius, S. Juršėnas and K. Kazlauskas, *J. Mater. Chem. C*, 2019, **7**, 11522–11531.
- 8 R. K. Konidena, K. H. Lee and J. Y. Lee, *J. Mater. Chem. C*, 2019, **7**, 9908–9916.
- 9 C. Chan, L. Cui, J. U. Kim, H. Nakanotani and C. Adachi, *Adv. Funct. Mater.*, 2018, **28**, 1706023.
- 10 Y. Im, S. H. Han and J. Y. Lee, *J. Mater. Chem. C*, 2018, **6**, 5012–5017.
- 11 S. J. Woo, Y. Kim, M. J. Kim, J. Y. Baek, S. K. Kwon, Y. H. Kim and J. J. Kim, *Chem. Mater.*, 2018, **30**, 857–863.
- 12 J. A. Seo, Y. Im, S. H. Han, C. W. Lee and J. Y. Lee, *ACS Appl. Mater. Interfaces*, 2017, **9**, 37864–37872.
- 13 Z. Li, W. Li, C. Keum, E. Archer, B. Zhao, A. M. Z. Slawin, W. Huang, M. C. Gather, I. D. W. Samuel and E. Zysman-Colman, *J. Phys. Chem. C*, 2019, **123**, 24772–24785.
- 14 Z. Cheng, Z. Li, Y. Xu, J. Liang, C. Lin, J. Wei and Y. Wang, *ACS Appl. Mater. Interfaces*, 2019, **11**, 28096–28105.
- 15 S. J. Woo, Y. Kim, S. K. Kwon, Y. H. Kim and J. J. Kim, *ACS Appl. Mater. Interfaces*, 2019, **11**, 7199–7207.
- 16 P. Rajamalli, D. Chen, W. Li, I. D. W. Samuel, D. B. Cordes, A. M. Z. Slawin and E. Zysman-Colman, *J. Mater. Chem. C*, 2019, **7**, 6664–6671.
- 17 Y. H. Lee, S. Park, J. Oh, S.-J. Woo, A. Kumar, J.-J. Kim, J. Jung, S. Yoo and M. H. Lee, *Adv. Opt. Mater.*, 2018, **6**, 1800385.
- 18 D. H. Ahn, S. W. Kim, H. Lee, I. J. Ko, D. Karthik, J. Y. Lee and J. H. Kwon, *Nat. Photonics*, 2019, **13**, 540–546.
- 19 S. Sun, R. Guo, Q. Zhang, X. Lv, P. Leng, Y. Wang, Z. Huang and L. Wang, *Dye. Pigment.*,

- 2020, **178**, 108367.
- 20 V. V. Patil, K. H. Lee and J. Y. Lee, *Dye. Pigment.*, 2020, **174**, 108070.
- 21 R. Huang, N. A. Kukhta, J. S. Ward, A. Danos, A. S. Batsanov, M. R. Bryce and F. B. Dias, *J. Mater. Chem. C*, 2019, **7**, 13224–13234.
- 22 D. Song, Y. Yu, L. Yue, D. Zhong, Y. Zhang, X. Yang, Y. Sun, G. Zhou and Z. Wu, *J. Mater. Chem. C*, 2019, **7**, 11953–11963.
- 23 L.-S. Cui, H. Nomura, Y. Geng, J. U. Kim, H. Nakanotani and C. Adachi, *Angew. Chemie Int. Ed.*, 2017, **56**, 1571–1575.
- 24 T. Serevičius, R. Skaisgiris, I. Fiodorova, V. Steckis, J. Dodonova, D. Banovičius, K. Kazlauskas, S. Juršėnas and S. Tumkevičius, *Org. Electron.*, 2020, 105723.
- 25 M. Kim, S. K. Jeon, S.-H. Hwang and J. Y. Lee, *Adv. Mater.*, 2015, **27**, 2515–2520.
- 26 I. Lee and J. Y. Lee, *Org. Electron.*, 2016, **29**, 160–164.
- 27 S. Wu, M. Aonuma, Q. Zhang, S. Huang, T. Nakagawa, K. Kuwabara and C. Adachi, *J. Mater. Chem. C*, 2014, **2**, 421–424.
- 28 R. Komatsu, T. Ohsawa, H. Sasabe, K. Nakao, Y. Hayasaka and J. Kido, *ACS Appl. Mater. Interfaces*, 2017, **9**, 4742–4749.
- 29 Y. Wada, S. Kubo and H. Kaji, *Adv. Mater.*, 2018, **30**, 1705641.
- 30 N. Jürgensen, A. Kretzschmar, S. Höfle, J. Freudenberg, U. H. F. Bunz and G. Hernandez-Sosa, *Chem. Mater.*, 2017, **29**, 9154–9161.
- 31 M. Y. Wong, S. Krotkus, G. Copley, W. Li, C. Murawski, D. Hall, G. J. Hedley, M. Jaricot, D. B. Cordes, A. M. Z. Slawin, Y. Olivier, D. Beljonne, L. Muccioli, M. Moral, J. C. Sancho-Garcia, M. C. Gather, I. D. W. Samuel and E. Zysman-Colman, *ACS Appl. Mater. Interfaces*, 2018, **10**, 33360–33372.
- 32 X. Liang, H. B. Han, Z. P. Yan, L. Liu, Y. X. Zheng, H. Meng and W. Huang, *New J. Chem.*, 2018, **42**, 4317–4323.